13th World Conference on Earthquake Engineering
Vancouver, B.C., Canada
August 1-6, 2004
Paper No. 1883

TENSILE CONNECTED BRACE WITH WEDGE DEVICE FOR PERFORMANCE-BASED SEISMIC DESIGN

Takao TAKAMATSU [1], Hiroyuki TAMAI [2] and Akihiro KOMOCHI [3]

SUMMARY

This paper proposes a brace whose strength, remaining plastic deformation capacity and energy absorption capacity can be easily evaluated under seismic loading, considering performance-based seismic design. The proposed brace consists of a slender rod with tensile-connected ends incorporating a tapered washer and wedge. There is no buckling in the brace. The wedge slides between washer and stand so as to prevent brace looseness due to axial plastic deformation under repeated loading.

To verify the brace's mechanism and performance, repeated horizontal loading tests were performed on a one-story bay frame with a tensile connected brace having a wedge device.

Results and conclusions obtained from loading tests are summarized as follows.

1) Perfect elasto-plastic hysteresis was observed until the wedge's slide displacement reached its maximum. 2) Story shear stiffness, strength and energy absorption capacity were easily evaluated. 3) Plastic deformation capacity remaining after an earthquake can be evaluated by checking the wedge's total sliding displacement. 4) Performance-based design can be easily achieved with this brace.

INTRODUCTION

The Japanese seismic code was revised as performance-based design in 2000.

An important task in performance-based seismic design is the characterization of maximum story drifts induced into building frames under a given earthquake level, because the maximum story drift has been regarded as the primary index for assessing the degree of damage. For tall buildings, the optimum story shear strength distribution is set to prevent damage concentration in a story and to reduce the maximum story drift under severe earthquake ground motion.

To guarantee safe maximum story drift, the strength and second branch stiffness after yielding in each story must be set accurately [1,2]. Furthermore, it is desirable to easily evaluate remaining seismic resistance capacity and to determine the need to repair members after an earthquake [3]. Structural

[1] Professor, Faculty of Engineering, Hiroshima Institute of Technology, Ph.D., takamatsu@cc.it-hiroshima.ac.jp

[2] Associate Professor, Faculty of Engineering, Hiroshima Institute of Technology, Dr. of Eng., tamrix@cc.it-hiroshima.ac.jp

[3] Structural Engineer, ADO Architectural Design Office, Mr. of Eng.

members that specify the seismic performance of a building are horizontal-force-resisting members such as braces.

In recent years, hysteretic dampers that reduce the seismic response of a building have been developed by many researches [4-7]. In general, the fundamental structural parameters, such as strength and second branch stiffness after yielding, of hysteretic dampers subjected to repeated loading are very difficult for ordinary engineers to evaluate. This is because the joint, shape and mechanism of the dampers are complicated.

Thus, this paper proposes a simple brace as a hysteretic damper, whose strength, second branch stiffness after yielding, remaining plastic deformation capacity and energy absorption capacity can be easily evaluated under seismic loading.

MECHANISM AND SPECIAL FEATURES OF NON-COMPRESSION BRACE TOWARD PERFORMNCE-BASED SEISMIC DESIGN

The proposed braced frame is shown in Figure 1. Details of the device at the end of the brace are shown in Figure 2. The proposed brace consists of a slender rod with a tensile-connected end with a tapered washer and wedge. We call it a “non-compression brace” hereafter. There is no buckling in the brace, because no compressive axial force acts on it under severe earthquake ground motion. The wedge slides between washer and stand so as to prevent looseness of brace due to axial plastic deformation under repeated horizontal loading.

Using the non-compression brace, whose strength under repeated loading is easily determined, perfect elasto-plastic hysteresis is obtained because the full length of the rod except the screw joint yields uniformly without strain hardening. Hence, the plastic deformation capacity is enough for the braced frame under severe earthquake ground motion. Furthermore, the energy absorption capacity is specified by means of the maximum slide length of the wedge. In addition, there is no need for pre-tensioning during building construction to obtain high story shear stiffness, because the brace has a self-tensioning mechanism under external turbulences such as winds.

For performance–based seismic design using hysteretic dampers, it is required to precisely set the elastic limit story shear strength, story drift and story shear stiffness after yielding for each design value. It is also desirable to evaluate the remaining energy absorption capacity after an earthquake.

Using the present brace, these requirements are easily satisfied as shown above.

In the following section, to show the brace’s mechanism and performance, repeated horizontal loading tests are performed on a one-story bay frame with a tensile connected brace having a wedge device.

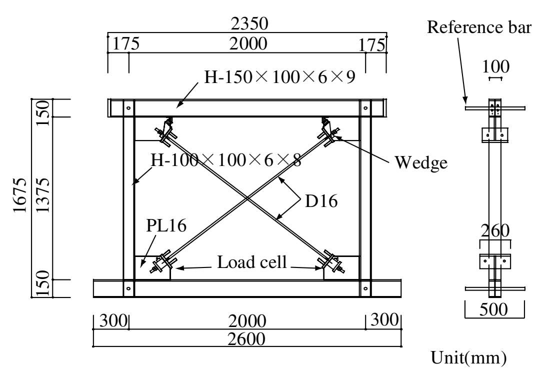

Figure 1 Test specimen (Present braced frame).

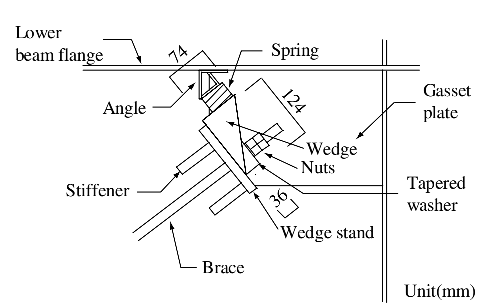

Figure 2 Device of connection in end of brace.

SHAPE REQUIREMENT OF WEDGE AND WASHER

To effectively absorb the seismic energy into the plastic deformation of the rod, it is required to stick the wedge and the tapered washer when tensile axial force acts on the brace. Now, we consider the equilibrium of the tapered washer and wedge subjected to compressive force from the rod (See Figure 4). Friction force and normal force on the surface between the tapered washer and wedge, *F, N* are written as follows:

$$N=P\cos\theta,\quad S=P\sin\theta \qquad (1.a,b)$$

P and θ denote the compressive force from the rod and the taper angle of the washer and wedge, respectively. Using friction coefficient μ, friction force *F* is written as:

$$F=\mu N \qquad (2)$$

To avoid washer slip-back, the following condition must be satisfied.

$$F > S \qquad (3.a)$$

By substituting equations (1.a, b), (2) into equation (3.a), we obtain:

$$\theta < \tan^{-1}\mu \qquad (3.b)$$

From the experimental results shown in Table 2, the minimum friction coefficient of the wedge is 0.70. There is no slip if we choose a taper angle below 0.611 *rad*. Hence, we choose a taper angle of washer and wedge of 0.532 *rad*.

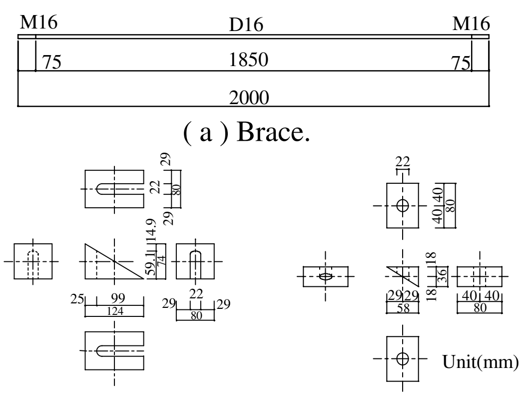

(b) Wedge. (c) Tapered washer.

Figure 3 (a),(b),(c) Detail of brace, wedge and tapered washer.

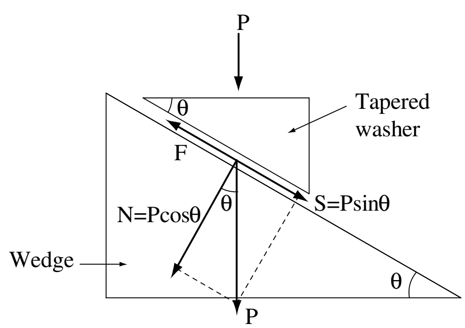

Figure 4 Equilibrium of wedge and tapered washer.

Table 1 Mechanical properties of materials.

Point of material	E kN/mm^2	σ_y N/mm^2	σ_u N/mm^2	σ_y/σ_u	ε_{st} %	ε_f %
Brace	205	318	453	0.68	2.36	26
Beam and Column	205	318	436	0.72	2.34	29

E : Young's modulus, σ_y: Yield stress

σ_y : Tensile strength, σ_y/σ_u : Yield ratio

ε_{st} : Strain at hardening observed after yielding

ε_f : Fracture strain (Elongation)

Table 2 Surface roughnesses for wedges.

	No.1	No.2	No.3	No.4
Friction coefficient	0.939	0.932	0.701	0.718

OUTLINE OF TESTS

Test Apparatus

The specimen is shown in Figures 1,2. The test specimen is a one-story bay frame with the present braces. The braces are tension-connected braces with a wedge device at their ends. The wedge device consists of a wedge with 0.532 *rad* angle, a tapered washer, a wedge stand and a spring. Details of the brace, wedge and tapered washer are shown in Figure3. The test setup is shown in Figure 5. The specimen was fastened to a reaction frame. Two digital jacks were joined to the beam of the specimen through a reaction beam. During tests, tensile and compressive horizontal forces acted on the specimen.

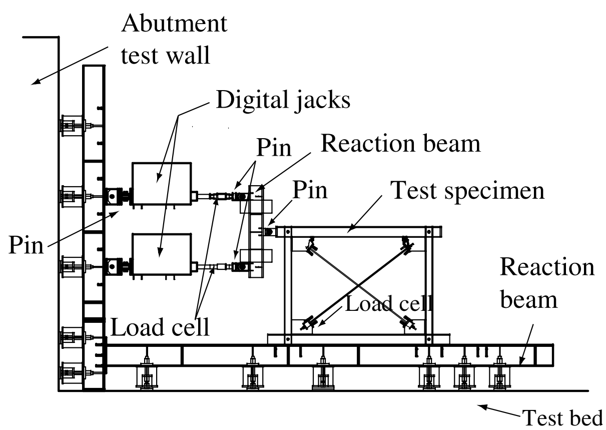

Figure 5 Test apparatus.

Measurements

Loading measurements were horizontal forces acted on the whole specimen and frame, Q and Q_f, and axial force in braces in left-lower to right-upper and right-lower to left-upper directions, T_L and T_R. Q, T_L and T_R were measured by load cells. Q_f was derived from strains at the tops and bottoms of columns as follows.

$$Q_f = (M_a - M_a^*)/L_a - (M_b - M_b^*)/L_b \tag{4}$$

Where, (M_a, M_a^*), (M_b, M_b^*) are bending moments at tops and bottoms of left and right side columns. L_a and L_b are the distance between evaluation points of bending moment in the left and right side columns. Bending moments were calculated from strains at both edges of column section, ε_T, ε_B.

$$M = -E\,I\,\kappa \tag{5.a}$$

Where,

$$\kappa = (\varepsilon_T - \varepsilon_B)/D \tag{5.b}$$

EI and D are flexural rigidity and height of column section.

Horizontal force due to brace, Q_b, was derived as follows.

$$Q_b = Q - Q_f \tag{6}$$

Displacement measurements were inter-story drift, Δ, wedge slide displacement, δ_s, left-lower to right-upper and right-lower to left-upper diagonal displacements, δ_L, δ_R. Δ, δ_s, δ_L and δ_R were averaged values from the front and the rear instruments. Strain measurements were brace strains at the left-lower end, center and right-upper end, ε_L, ε_M and ε_R. These measurement values are shown in Figure 6.

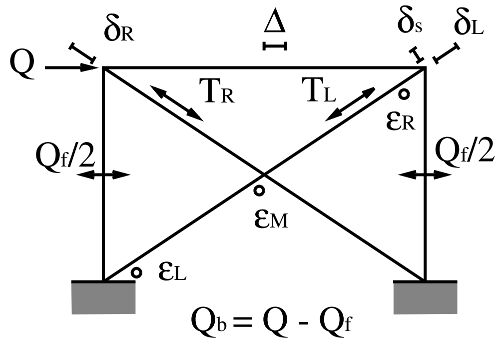

Figure 6 Schematic illustrations of measured values.

Loading Programs

Loading programs were single level cyclic loading which the amplitude were constant to Δ/H=1/1000 *rad* (Case I) and Δ/H=1/150 *rad* (Case II). In both cases, braces pretensions were set to 9.0 *kN*.

TEST RESULTS AND DISCUSSION

Test results are shown in Figures 7-12 and Photograph 1.

Figs.7 and 8 show the test results of Case I. Fig.7 shows the horizontal force due to the brace normalized by its yield load, Q_b/Q_{by}, vs. inter-story drift normalized by drift when the brace is yielding, Δ/Δ_y, relation. Fig.8 shows the axial force in the left-lower to right-upper and right-lower to left-upper diagonal braces normalized by their fully plastic axial force, T_L/T_{Ly} and T_R/T_{Ry}, vs. elongation of left-lower to right-upper and right-lower to left-upper diagonal braces normalized by their yield elongation, δ_L/δ_{Ly} and δ_R/δ_{Ry}, relations.

Figs.9-12 and Photo.1 show test results of Case II.

Fig.9 shows the Q_b/Q_{by} vs. Δ/Δ_y relation. Fig.10 shows the (T_L/T_{Ly}) vs. (δ_L/δ_{Ly}) and (T_R/T_{Ry}) vs. (δ_R/δ_{Ry}) relations as in Fig.8. Fig.11 shows (T_L/T_{Ly}) vs. strain at the left-lower end, center and right-upper end of the brace, ε_L, ε_M and ε_R relations. Also, Fig.12 shows horizontal force for overall specimen normalized by horizontal force when the brace is yielding, Q/Q_y, vs. wedge slide displacement normalized by its maximum slide displacement, δ_s/D_w relation. In Figs.9-12, the loading stages are described in capitals from A to J.

Photo.1 shows the movement of the wedge at the right-upper corner of the frame in A,D,J,I loading stages.

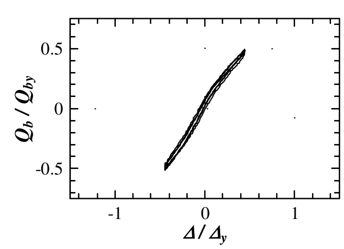

Figure 7 (Q_b/Q_y) vs. (Δ/Δ_y) relation in Case I.

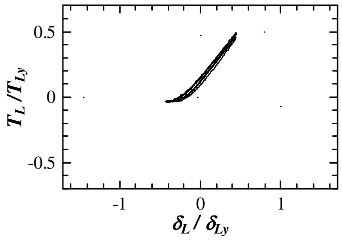

(a) (T_L/T_{Ly}) - (δ_L/δ_{Ly}).

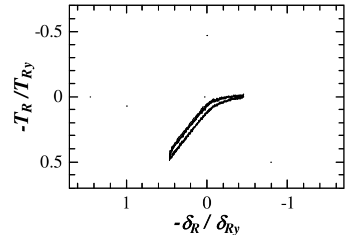

(b) (T_R/T_{Ry}) - (δ_R/δ_{Ry}).

Figure 8(a),(b) Axial force vs. elongation for brace in Case I.

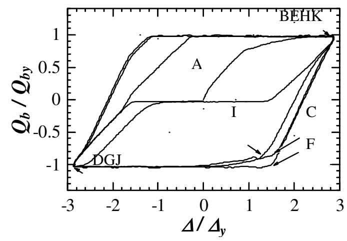

Figure 9 (Q_b/Q_y) vs.(Δ/Δ_y) relation in Case II.

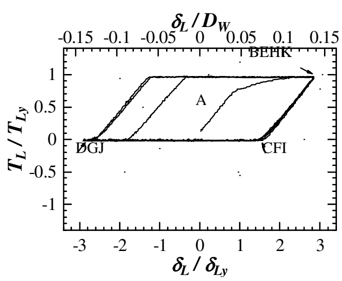

(a) (T_L/T_{Ly}) - (δ_L/δ_{Ly}).

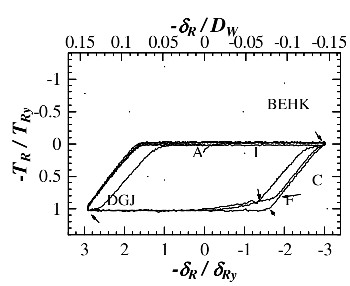

(b) (T_R/T_{Ry}) - (δ_R/δ_{Ry}).

Figure 10(a),(b) Axial force vs. elongation for brace in Case II.

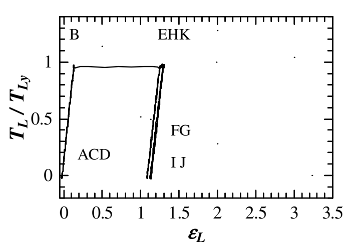

(a) Left-lower end.

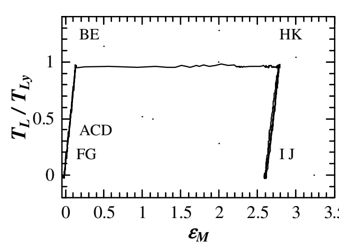

(b) Center.

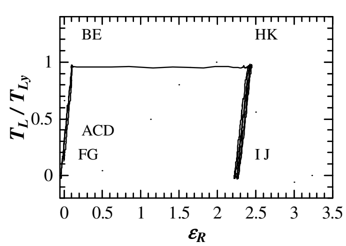

(c) Right-upper end

Figure 11(a),(b),(c) Axial force vs. strain relation for brace in Case II.

These results show the following items:

Elastic story shear stiffness

Figs.7 and 8 show the following regarding elastic stiffness of the brace:
i) The brace had high axial stiffness under tensile axial force. Conversely, when the axial force became zero, the axial stiffness disappeared.
ii) When axial force acted on the braces, high axial stiffness can be expected of both. Hence, elastic story shear stiffness was higher than for a diagonal brace.
iii) Horizontal load due to brace vs. inter-story drift relation can be assumed to be S-shaped tri-linear under elastic response.
Hence, elastic story shear stiffness due to the brace can be evaluated from single brace stiffness where the brace pretensions are relatively small.

Elasto-plastic restoring force characteristics

Figs.9,10 and 12 show the following regarding elasto-plastic behavior of the brace:
i) Story shear strength due to the brace at virgin yielding was 20% less than calculated strength, Q_{by}.
ii) Story shear stiffness due to the brace under unloading was twice the initial story shear stiffness.
iii) The story shear force due to the brace, Q_b/Q_y vs. story drift, Δ/Δ_y, relation showed perfect elasto-plastic hysteresis, from which the strength under repeated loading is easily determined.
iv) After 4 cycles, the (Q_b/Q_y) vs. (Δ/Δ_y) relation showed slip hysteresis, showing that the restoring force characteristics deteriorated. This phenomenon caused the wedge slip displacement to reach its maximum displacement.

Plastic deformation of brace member

Figs.10, 11 show following items regarding plastic deformation of the brace.
i) Although development of plastic strain differed among left-lower end, center and right-upper end of the brace, overall yielding in the braces was observed.
ii) No strain hardening was observed during the test.
As overall brace yielding is occurring, the brace has enough plastic deformation capacity even if we use cutting thread braces.

Wedge penetration characteristics

Figs.10 and 12 and Photo.1 show the following regarding movement of the wedge under loading.
i) Wedge slip displacement increased when brace axial force varied from positive to zero.
ii) Increment of wedge slip displacement in a loading cycle path C-D, F-G coincided with increment of brace plastic deformation in the same loading cycle.
iii) Within 3 cycles, the wedge slid smoothly between washer and stand. The wedge was not pushed back when tensile axial force acted on the brace.
iv) After 3 cycles, wedge displacement reached its maximum. The braces became loose due to their plastic elongation. Restoring force characteristics of braces deteriorated.
Hence, the plastic absorption capacity of the present brace was governed by maximum wedge slip displacement. In other words, the plastic absorption capacity can be easily evaluated from the total slip displacement of the wedge.
It is clarified that the important variables for performance-based seismic design, such as elastic stiffness, elasto-plastic hysteresis, strength, plastic deformation and plastic absorption capacity, are easily evaluated with the present brace.

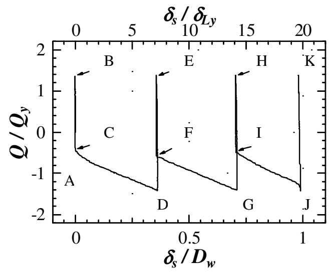

Figure 12 (Q/Q_y) vs. (δ_s/D_w) relation in Case II.

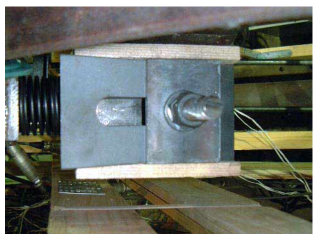

(a) Stage A.

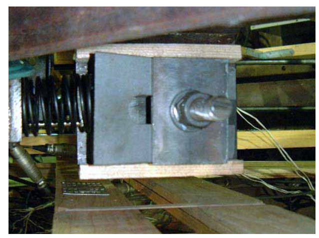

(b) Stage D.

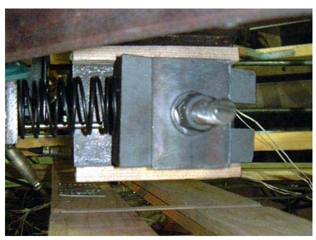

(c) Stage G.

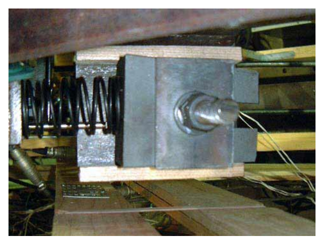

(d) Stage J.

Photograph 1 Appearance of right-upper corner wedge under loading test (Case II).

CONCLUDING REMARKS

We have proposed a non-compression brace that consists of a rod with tensile-connected ends with a tapered washer and a wedge. Repeated horizontal loading tests were performed on a one-story bay frame with a non-compression brace. Results and conclusion obtained from loading tests are summarized as follows.

1) Perfect elasto-plastic hysteresis occurs until the slide displacement of the wedge reaches its maximum.
2) Story shear stiffness, strength and energy absorption capacity are easily evaluated.
3) The plastic deformation capacity remaining after an earthquake can be evaluated by checking the total sliding displacement of the wedge.
4) Performance-based design can therefore be easily performed using the present brace,.

ACKNOWLEDGMENTS

This work was supported by a Grant-in-Aid from the Ministry of Education, Science and Culture of Japan (Assoc. Prof. H. Tamai, On Improved Seismic Brace considering Rehabilitation of Safe Shelter, No.15510152) and a Grant-in-Aid of Steel Building from Japan Iron and Steel Federation (Assoc. Prof. H. Tamai, 2002).
We thank Mrs. S. Kagawa and K. Fujii of the Hiroshima Institute of Technology, for their cooperation in carrying out the experiments.

REFERENCES

1. Y. Kanazawa, H. Tamai (2002), "On performance evaluation method for a building with hysteretic damper", *Journal of Constructional Steel* (in Japanese), Vol.10, (pp.435-442).
2. K. Inoue, S. Kuwabara (1998), "Optimum strength ratio of hysteretic damper", *Earthquake Engineering and Structural Dynamics*, Vol.27, (pp.577-588).
3. H.Tamai, K. Kondoh, M. Hanai (1998), "Very-low-cycle fatigue characteristics of hysteretic damper installed in K-Braced frame and its life prediction under severe seismic loading", *Proceedings of Fifth Pacific Structural Steel Conference*, Vol.1 (pp.353-358).
4. C. Higgins, J. Newall (2001), "Development of economical hysteretic dampers", *Proceedings of Passive Damper Structure Symposium*, (pp.193-201).
5. H. Tamai, K. Kondoh, M. Hanai (1999), "On Mechanism of X-braced frame with hysteretic damper and its elasto-plastic behavior (part1) Tension connected braced frame", *Journal of Structural and Construction Engineering, Architectural Institute of Japan* (in Japanese), No.515, (pp.139-146).
6. H. Tamai, K. Kondoh, M. Hanai (2001), "On Mechanism of X-braced frame with hysteretic damper and its elasto-plastic behavior (part2) Shear connected braced frame", *Journal of Structural and Construction Engineering, Architectural Institute of Japan* (in Japanese) , No.543, (pp.153-160).
7. H. Tamai, K. Kondoh, Y. Kitagawa, M. Hanai (2000), "Shape effect on seismic energy absorption capacity of hysteretic damper for K-braced frame", *Proceedings of 12th World Conference of Earthquake Engineering*, 2467 (CDROM).